Available online at www.sciencedirect.com

SciVerse ScienceDirect

Journal of the European Ceramic Society 32 (2012) 2581–2586

www.elsevier.com/locate/jeurceramsoc

Thermal shock resistance of polycrystalline cubic boron nitride

D. Carolan *, A. Ivanković, N. Murphy

School of Mechanical and Materials Engineering, University College Dublin, Ireland

Received 24 February 2012; accepted 11 March 2012
Available online 3 April 2012

Abstract

The effect of thermal shock on the flexural strength has been investigated experimentally. It was found that the variation in flexural strength with quench temperature was influenced by the CBN grain size. Polycrystalline material containing small CBN grains showed a discontinuous drop in measured flexural strength above a material dependent critical quench temperature difference, ΔT_c. The sharp decrease in measured strength is accompanied by unstable crack propagation. Material containing a significantly larger CBN grain size exhibited a gradual decrease in strength above the critical quench conditions. The experimental observations agreed with an established theory developed for thermal shock of alumina. The theoretically calculated critical temperatures agree well with the observed experimental data for each material when a flaw size equal to the CBN grain size is employed.

Keywords: Cubic boron nitride; Fracture; Thermal shock

1. Introduction

Polycrystalline cubic boron nitride (PCBN) is a super hard material used in the machining of hardened steels, aerospace grade alloys and other abrasive materials. [1–3] In these applications the tools are subjected to high operating temperatures, abrasion and impact loading. This can lead to the brittle fracture of the tool. Accurate determination of the fracture characteristics of PCBN under a wide range of loading rates and temperatures is therefore essential in order to evaluate the performance of the tool under these highly demanding operating conditions. The current work examines the thermal shock performance of two grades of PCBN.

Thermal shock occurs when a material is exposed to temperature extremes in a short period of time. Under these conditions, the material is not in thermal equilibrium, and internal stresses may be sufficient to cause fracture of the material. The ability to withstand thermal shock is a function of several variables, including the thermal conductivity, k, the coefficient of thermal expansion, α and the specific heat capacity, c_p. Winkleman and Schott[4] proposed an empirical parameter they called the coefficient of thermal endurance which gives a qualitative estimate of the ability of a material to withstand thermal shock.

$$E_{\text{th}} = \frac{F}{\alpha E}\sqrt{\frac{k}{\rho c_p}} \tag{1}$$

where E_{th} is the coefficient of thermal endurance, not to be confused with the Young's modulus E, which appears on the right hand side of Eq. (1) and F is the material tensile strength. Selected coefficients of thermal endurance are given in Table 1.[6] It is significant to note the large difference in thermal endurance between cubic boron nitride and a variety of typical PCBN binder phases. This is an indicator that fracture of polycrystalline cubic boron nitride may be a thermally controlled phenomenon.

A theoretical analysis of crack propagation in brittle ceramics under the influence of thermal stresses was conducted by Hasselman and co-workers.[5,7] They found that for a material with small cracks, which propagate kinetically on initiation, the crack length and material strength are expected to change with the severity of quench, shown schematically in Fig. 1. Specimens with initial crack lengths longer than some critical value were found to propagate stably. Further to this, Gupta[8] found for alumina of varying grain sizes the extent of unstable crack propagation was inversely proportional to the grain size of the material. More recently several researchers have applied the analysis to composite ceramic materials[9–12] as well as functionally graded

* Corresponding author. Tel.: +353 1716 1880; fax: +353 1283 0534.
E-mail address: declan.carolan@ucd.ie (D. Carolan).

0955-2219/$ – see front matter © 2012 Elsevier Ltd. All rights reserved.
doi:10.1016/j.jeurceramsoc.2012.03.013

Table 1
Thermal endurance factor for selected materials.

Material	E_{th}
Cubic boron nitride	648
Diamond (Type IIA)	30.29
Aluminium nitride	2.325
Silicon carbide	1.4
Alumina (99%)	0.640
Alumina (96%)	0.234

ceramics.[13] Whilst the importance of thermal shock resistance for PCBN cutting tool materials is widely acknowledged,[14,15] little or no attempt has been made to date to apply these existing theories to PCBN.

A significant result from the work by Hasselman[5] is the difference between resistance to crack initiation and resistance to crack propagation. Resistance to crack initiation, R', and crack propagation, R'', is given by:-

$$R' = \frac{GE}{\sigma_t^2(1-\nu)} = \frac{K^2}{\sigma_t^2(1-\nu)} \tag{2}$$

$$R'' = \sqrt{\frac{G}{\alpha^2 E}} = \frac{K}{\alpha E} \tag{3}$$

where G is the fracture energy, K is the stress intensity factor, E is the Young's modulus of the uncracked specimen and σ_t is the tensile strength of the material. It can be clearly seen that resistance to crack initiation is proportional to K^2 and inversely proportional to σ_t^2 whereas resistance to crack propagation is linearly proportional to K. Therefore a material will be more resistant to crack initiation if it has a larger fracture process zone size since most estimates of process zone size indicate a proportionality to $(K/\sigma)^2$,[16–18] whereas resistance to crack propagation is purely a function of toughness. The intrinsic strength of the material does not affect the material's ability to resist crack propagation.

Hasselman developed an analytical expression to calculate the critical temperature difference at which the flexural strength begins to decrease. For initial short cracks this is given as[5,19]:-

$$\Delta T_c = \left[\frac{\pi\gamma(1-2\nu)^2}{2E\alpha^2(1-\nu^2)^2}\right]^{1/2} c^{-1/2} \tag{4}$$

where γ is the energy required to create a new surface ($\gamma = G/2$), α is the linear expansion coefficient, E is the Young's modulus of an uncracked specimen, ν is the Poisson's ratio and c is the initial crack length.

2. Materials and methods

Rectangular specimens of length 28.5 mm, width 6.25 mm and thickness 4.76 mm were provided by Element 6 for testing. PCBN material is generally sintered under high temperature (1200–1500 °C), high pressure (4–7 GPa) conditions. Two grades of PCBN material were provided. The first grade, denoted PCBN A has a grain size of 22 μm, with 90 vol.% CBN grains.

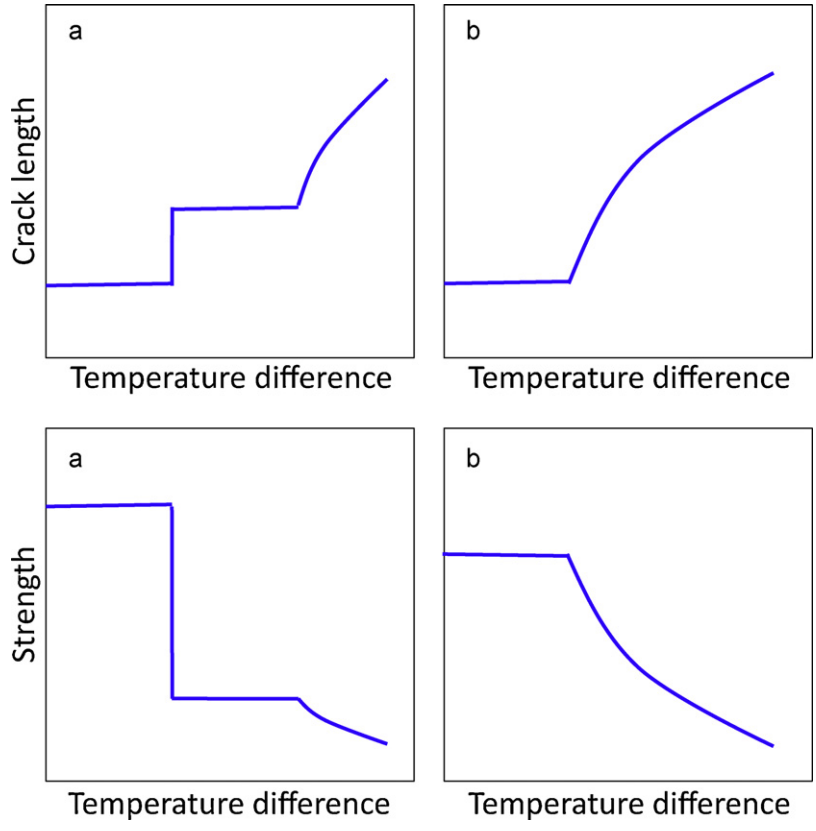

Fig. 1. Crack propagation and strength for unstable (a) and stable (b) crack propagation conditions.[5]

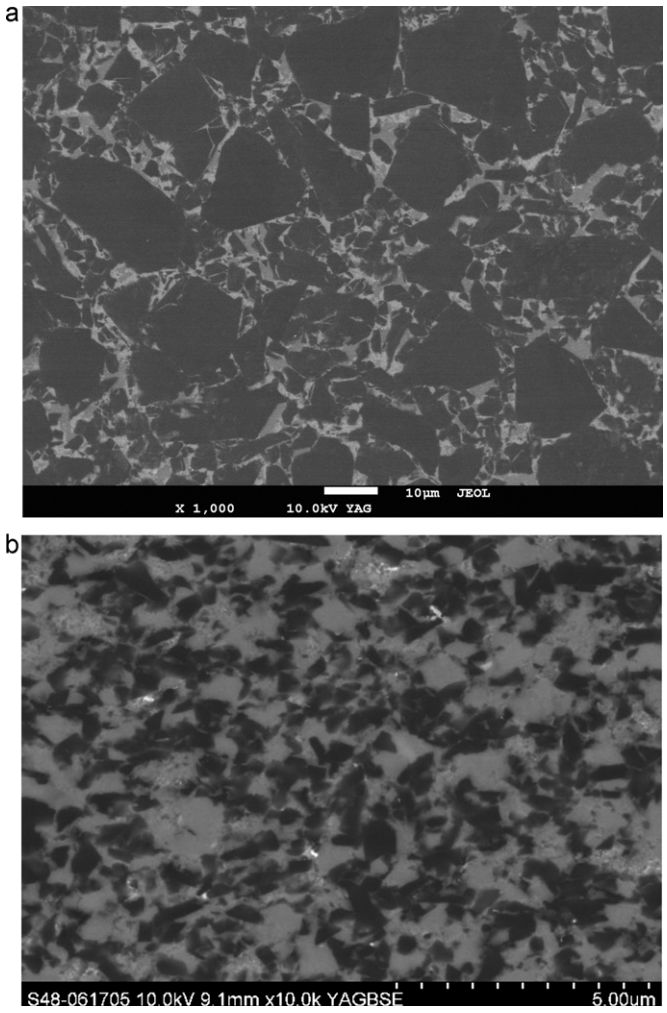

Fig. 2. Scanning electron micrographs of PCBN A and PCBN B showing CBN particles (dark phase).

The second grade, denoted PCBN B has a grain size of 1 μm with a lower volume percent of CBN, approximately 60%. The binder phase for PCBN A is best described as aluminium based ceramic, whilst for PCBN B the binder is a typical titanium carbo-nitride binder. Typical micrographs for the two materials under investigation are given in Fig. 2. Thermo-mechanical constants for the constituent materials of both PCBN A and PCBN B as are shown in Table 2.[20]

In total 84 samples were tested in three point bending, 46 for PCBN A and 46 for PCBN B. For each grade, 15 were samples

Table 2
Thermal properties of PCBN grades and binder constituents.[20]

	PCBN A	PCBN B
G_{PCBN} [J/m^2]	70	11
D [μm]	22	1
E_{CBN} [GPa]	800	800
ν_{CBN}	0.14	0.14
α_{CBN} [10^{-6}/K]	1.2	1.2
E_{binder} [GPa]	315	250
ν_{binder}	≈0.2	≈0.2
α_{binder} [10^{-6}/K]	4.8	9.4

Table 3
Approximate heat transfer coefficients for various media.[24]

Quench media	h [W/m^{2}K]
Water	5000
Oil	2000
Air	200

were tested in the *as-received* condition and a full Weibull analysis of the strength was carried out.[21] A full description of Weibull's method is given in Ref. [22] The important outputs from the analysis are the characteristic strength, σ_0 and the Weibull modulus, m, a measure of the degree of scatter of the data.

The flexural strength of each sample was calculated via Eq. (5) in accordance with BS-EN 843:1[23] where σ_f is the flexural strength, P_{in} is the breaking load, b is the width, h is the height and s is the span of the supporting rollers. The samples were loaded to fracture using a constant crosshead displacement rate of 1 mm/min.

$$\sigma_f = \frac{3P_{in}s}{2bh^2} \quad (5)$$

The remaining samples were then subjected to a variety of heat treatments, water quench with quench temperature difference, ΔT, varying between 220 °C and 1080 °C, oil quench, 220 °C <ΔT< 1080 °C and water quench with subsequent anneal. The oil used was a light grade oil. Approximate heat transfer coefficients for unagitated water, oil and air quenching are given in Table 3.[24]

For each heating cycle, samples were heated at a rate of 40 °C/min up to the required holding temperature and then held at that temperature for a period of 1 h. The annealing temperature in all cases was the same as the quench temperature and the anneal hold time was 2 h. After annealing, the samples

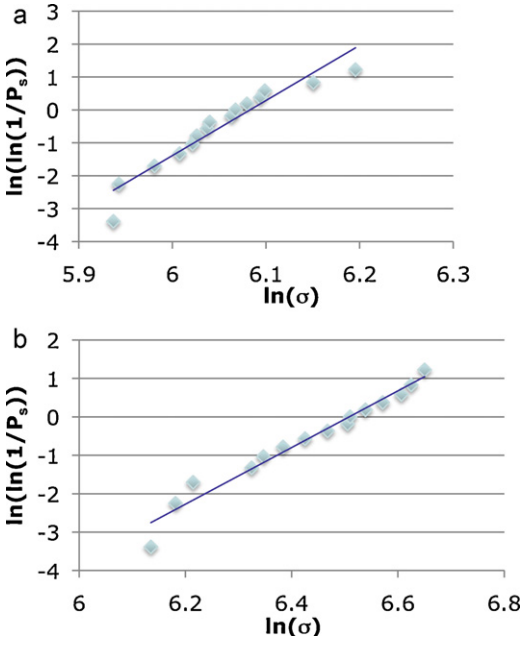

Fig. 3. Weibull plot of strength data for (a) PCBN A (n = 15, m = 15.7, σ_0 = 438 MPa) and (b) PCBN B (n = 15, m = 7.4, σ_0 = 670 MPa).

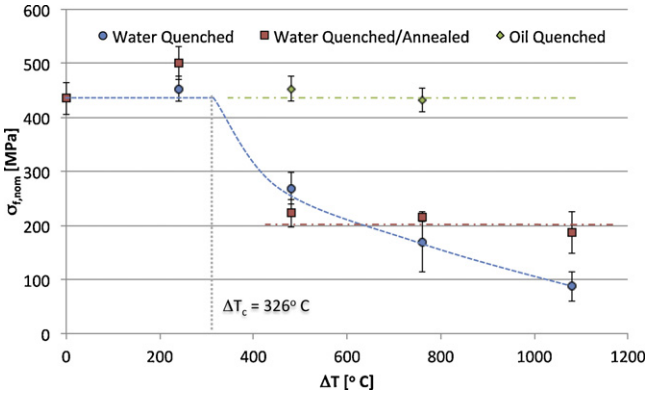

Fig. 4. Flexural strength of PCBN A quenched in water and subsequent annealing from quench temperature as a function of quench temperature difference [ΔT].

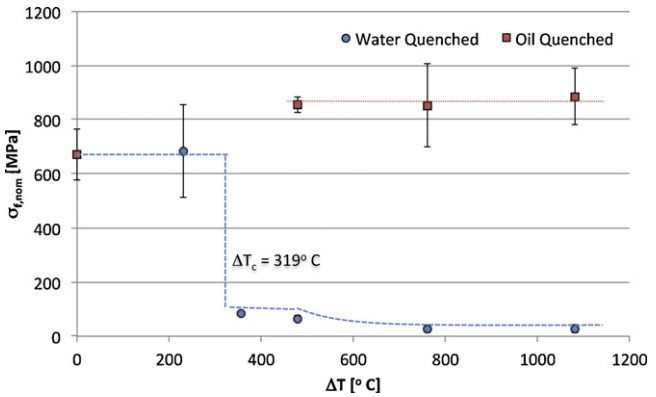

Fig. 5. Flexural strength of PCBN B quenched in oil and water as a function of quench temperature difference [ΔT]. The standard deviations of strength values for quenched material $>T_c$ are sufficiently small as to be hidden in the figure.

were allowed to cool slowly in the closed furnace. They were subsequently fractured in three point bend using the method previously described.

3. Results and discussion

Flexural strength results for both grades of PCBN investigated are presented in Fig. 3. The Weibull modulus, m, was lower for PCBN B, $m = 7.4$, than for PCBN A, $m = 15.7$, indicating a greater scatter in strength data for the smaller grained material.

Figs. 4 and 5 present the results of the various heat treatments, oil quench, water quench and water quench with subsequent annealing from the quench temperature on both PCBN A and PCBN B. PCBN A exhibits stable crack propagation for water annealing at all levels of quench as explained in Fig. 1. The maximum quench temperature difference, 1080 °C, resulted in a drop in strength to 87.6 MPa, 20% of the *as-received* value. Oil quenching had no effect on the measured flexural strength of PCBN A.

An oil quench on PCBN B has the effect of increasing the average flexural strength. The oil quench, which is a less severe quench than a water quench, may have had the effect of relieving the existing residual stress field, caused by the sintering and machining of the sample.

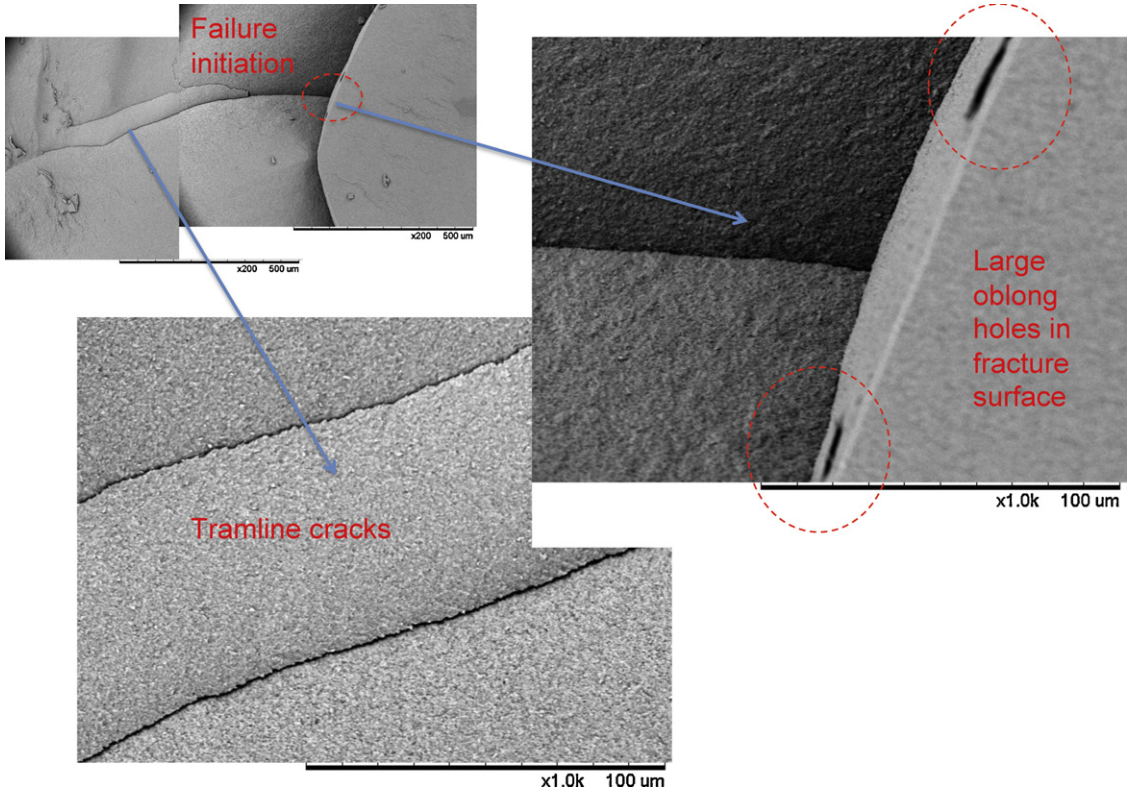

Fig. 6. SEM micrographs showing main features of quench failure of PCBN B.

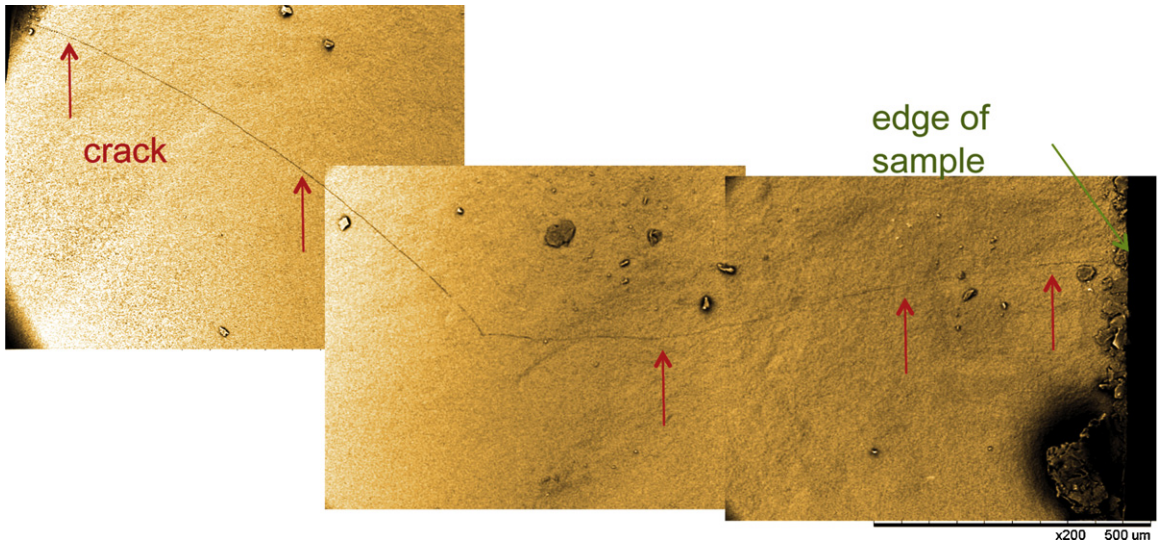

Fig. 7. Knitted SEM micrograph of long unopened crack extending from failure initiation region to edge of sample.

A severe water quench causes a large discontinuous drop in flexural strength for a quench temperature difference of between those samples quenched through 375 °C and above. This type of behaviour can be termed unstable crack growth as explained previously in Fig. 1. Below 240 °C no drop in flexural strength was recorded. The flexural strength recorded for a quench temperature difference of 780 °C and above was very low, (≈ 25 MPa). It was noted that the failure was very low energy and the fracture initiated from the centre of the sample. This is clearly illustrated in Fig. 6. The failed material also exhibited long unopened cracks extending from the initiation site to the edge of the sample as shown in Fig. 7. A significant surface colour change was also noted on quenching at these temperatures, from dark grey to light blue and upon microscopic investigation, significant voids close to the surface were noted as shown in Fig. 8. It is thought that this colour change is a result of the oxidation of the titanium based binder near the surface. This has not been investigated further in this work.

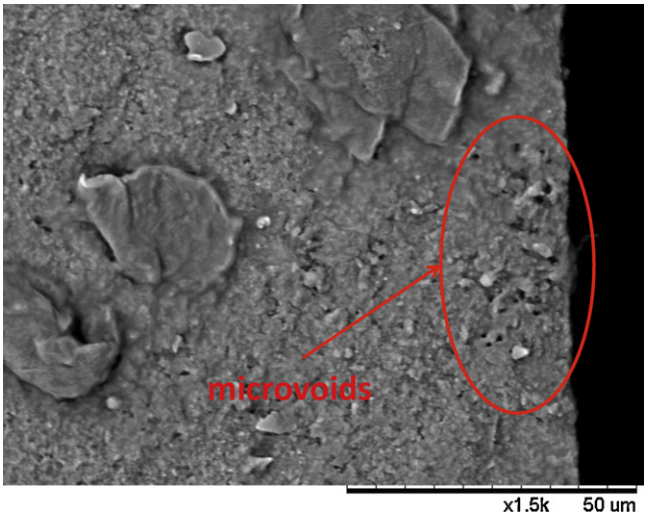

Fig. 8. Fracture surface of PCBN B flexural strength sample, quenched from 1100 °C. Microscopic voids are clearly evident close to the surface which are not present in the unquenched sample. (For interpretation of the references to colour in this figure legend, the reader is referred to the web version of this article.)

It was found that simply heating either material up to a temperature following by slow cooling in the furnace showed no change in the measured value of flexural strength for PCBN B. Therefore furnace heating alone does little to anneal the residual stresses and there exists some intermediate rate of cooling which appears to be beneficial in terms of the measured flexural strength at least for PCBN B.

Using the thermal properties for the binders in both cases from Table 2 in conjunction with Eq. (4), it is found that for an initial crack length, c, equal to the average CBN grain size, D, of the material, ΔT_c= 326 °C for PCBN A and 319 °C for PCBN B. This prediction agrees with the experimental data shown in Figs. 4 and 5. If, on the other hand, the critical temperature is calculated using the thermal properties of the CBN grains, ΔT_c = 1070 °C for PCBN A and 1990 °C for PCBN B. The available data on the thermal properties of the composite materials, i.e. binder and CBN together, are obtained under steady-state experimental conditions and do not take account of any transient behaviour which may occur for short time intervals. It is important to note that the thermal properties presented in Table 2 are room temperature values. However work by Carolan[25] has shown that the bulk thermoelastic properties of both PCBN A and PCBN B are not significantly affected by a global increase in temperature up to 800 °C. Thus, the use of room temperature properties in the thermal shock calculations is justified.

4. Conclusion

The thermal shock resistance of two grades of PCBN material was determined experimentally by measuring the flexural strength of the material after being subjected to a quench treatment. It was found that the thermal shock resistance of the material was governed by the thermal properties of the binder phase and not by the thermal properties of either the

composite materials or the CBN grains. However the size of the CBN grains plays an important role in determining the type and extent of crack propagation. It was shown that the crack can propagate either kinetically or quasi-statically depending on the initial crack length. Excellent agreement was found with an existing theory of thermal shock developed for monophase materials if the initial crack length was assumed to be a flaw of one CBN grain in length. Microscopic examination of fracture surfaces revealed that the locus of failure for severely quenched material was located in the centre of the specimen where tensile residual stresses are known to occur as a result of the rapid cooling. It is concluded that the theory developed by Hasselman sufficiently describes the thermal shock characteristics of PCBN.

Acknowledgements

The authors are grateful to Dr. Alun Carr and Dr. Kenneth Stanton for helpful discussions. This research was made possible by the financial support of *Element 6 Ltd, The Irish Research Council for Science, Engineering and Technology* and *Enterprise Ireland*.

References

1. Heath P. Properties and uses of Amborite. *Carbide and Tool Journal* 1987;**19**(2):12–22.
2. Fleming M, Wickham A. PCBN in the automotive industry. *Industrial Diamond Review* 2006;**2**:26–32.
3. Cook M, Bossom P. Trends and recent developments in the material manufacture and cutting tool application of polycrystalline diamond and polycrystalline cubic boron nitride. *International Journal of Refractory Metals and Hard Materials* 2000;**18**:147–52.
4. Winkleman A, Schott O. Ueber thermische widerstaas-scoefficienten verschnieder glaser in iherer Abhangigkei von der chemischen zusammensetzung. *Ann'n Phys Chem* 1894;**51**:1893–4.
5. Hasselman D. Unified theory of thermal shock fracture initiation and crack propagation in brittle ceramics. *Journal of the American Ceramic Society* 1969;**52**:600–4.
6. Harper C. *Handbook of Ceramics, Glasses and Diamonds*. New York: Mc Graw Hill; 2001.
7. Larson D, Coppola J, Hasselman D, Bradt R. Fracture toughness and spalling behaviour of high Al_2O_3 refractories. *Journal of the American Ceramic Society* 1974;**57**:417–21.
8. Gupta T. Strength degradation and crack propagation in thermally shocked Al_2O_3. *Journal of the American Ceramic Society* 1972;**55**: 249–53.
9. Aksel C, Warren PD. Thermal shock parameters [R′, R″' and R‴] of magnesia-spinel composites. *Journal of the European Ceramic Society* 2003;**23**:301–8.
10. Wang L, Shi JL, Gao JH, Yan DS. Influence of tungsten carbide particles on resistance of alumina matrix ceramics to thermal shock. *Journal of the European Ceramic Society* 2001;**21**:1213–7.
11. Chen JK, Tang KL, Chang JT. Effects of zinc oxide on thermal shock behavior of zinc sulfide-silicon dioxide ceramics. *Ceramics International* 2009;**35**:2999–3004.
12. Zhou XQ, Si TZ, Liu N, Ren PP, Xu YD, Feng JP. Effect of grain size on thermal shock resistance of Al_2O_3–TiC ceramics. *Ceramics International* 2005;**31**:33–8.
13. Zhao J, Ai X, Deng J, Wang J. Thermal shock behaviours of functionally graded ceramic tool materials. *Journal of the European Ceramic Society* 2004;**24**:847–54.
14. Wayne SF, Buljan ST. The role of thermal shock on tool life of selected ceramic cutting tool materials. *Journal of the American Ceramic Society* 1989;**72**(5):754–60.
15. Zhao J, Ai X, Huang XP. Relationship between the thermal shock behaviour and the cutting performance of a functionally gradient ceramic tool. *Journal of Materials Processing Technology* 2002;**129**:161–6.
16. Irwin G. Structural aspects of brittle fracture. *Applied Materials Research* 1964;**3**:65–81.
17. Ando K, Kim B, Iwasa M, Ogura N. Process zone size failure criterion and probabilistic fracture assessment curves for ceramics. *Fatigue and Fracture of Engineering Materials and Structures* 1992;**15**: 139–49.
18. Anderson T. *Fracture mechanics–fundamentals and applications*. 2nd Edition Boca Raton: CRC Press; 1995.
19. Kingery W, Bowen H, Uhlmann D. *Introduction to ceramics*. 2nd Edition New York: John Wiley and Sons; 1976.
20. Riedel R. *Handbook of ceramic hard materials, vol. 2*. Weinheim: Wiley VCH; 2000.
21. Weibull W. A statistical distribution function of wide applicability. *Journal of Applied Mechanics* 1951;**18**:293–7.
22. Wachtman JB. *Mechanical properties of ceramics*. New York: John Wiley and Sons; 1996.
23. BSI, Advanced Technical Ceramics–Mechanical properties of monolithic ceramics at room temperature. PArt 1: Determination of flexural strength. BS 843-1, British Standards Institution, 2006.
24. ASM International, ASM Handbook vol. 4: Heat Treating, 2nd Edition, 1994.
25. D. Carolan, Mechanical and Fracture Properties of Polycrystalline Cubic Boron Nitride as a Function of Rate and Temperature, PhD Thesis, University College Dublin, 2011.